

NANO EXPRESS

Open Access



Anisotropic Magnetoresistance of Nano-conductive Filament in Co/HfO₂/Pt Resistive Switching Memory

Leilei Li^{1,2}, Yang Liu³, Jiao Teng^{1*}, Shibing Long^{2,4,5*}, Qixun Guo¹, Meiyun Zhang^{2,4,5}, Yu Wu¹, Guanghua Yu¹, Qi Liu^{2,4,5}, Hangbing Lv^{2,4,5} and Ming Liu^{2,4,5}

Abstract

Conductive bridge random access memory (CBRAM) has been extensively studied as a next-generation non-volatile memory. The conductive filament (CF) shows rich physical effects such as conductance quantization and magnetic effect. But so far, the study of filaments is not very sufficient. In this work, Co/HfO₂/Pt CBRAM device with magnetic CF was designed and fabricated. By electrical manipulation with a partial-RESET method, we controlled the size of ferromagnetic metal filament. The resistance-temperature characteristics of the ON-state after various partial-RESET behaviors have been studied. Using two kinds of magnetic measurement methods, we measured the anisotropic magnetoresistance (AMR) of the CF at different temperatures to reflect the magnetic structure characteristics. By rotating the direction of the magnetic field and by sweeping the magnitude, we obtained the spatial direction as well as the easy-axis of the CF. The results indicate that the easy-axis of the CF is along the direction perpendicular to the top electrode plane. The maximum magnetoresistance was found to appear when the angle between the direction of magnetic field and that of the electric current in the CF is about 30°, and this angle varies slightly with temperature, indicating that the current is tilted.

Keywords: Conductive bridge random access memory, Resistive switching, Conductive filament, Anisotropic magnetoresistance

Background

In recent years, the requirements for non-volatile become more and more strict in the storage density, operation speed, and power consumption [1–7]. Resistive Random Access Memory (RRAM), which has the advantages of high integration, low power consumption, high read-write speed, and compatibility with CMOS technology, is regarded as one of the most promising new memories [8–10]. RRAM is based on the reversible switching between high and low resistance states (HRS and LRS) of a metal/insulator/metal structure in response to the external electric field [11, 12]. According to the difference of the electrode and switching mechanism, the

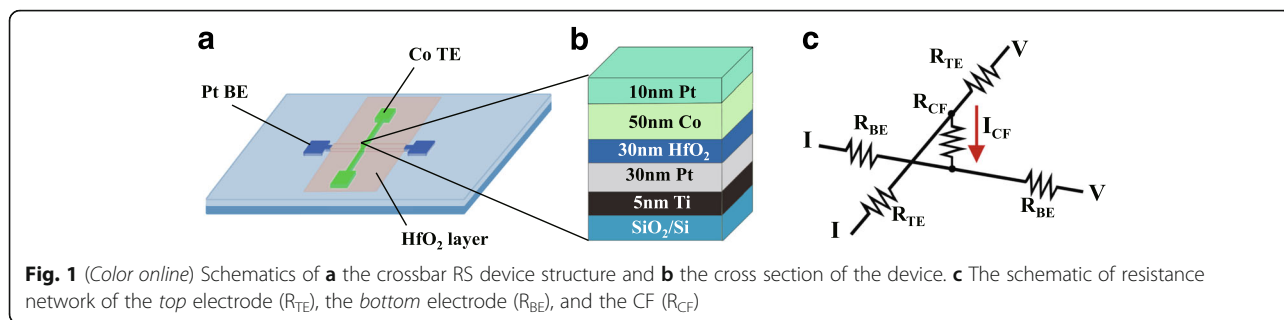
metal-oxide RRAM can be divided into electrochemical metallization memory (ECM) and valence change memory (VCM) [13, 14]. The ECM device is also called conductive bridge random access memory (CBRAM). In CBRAM, the SET and RESET switchings are attributed to the connection and rupture of metallic conducting filaments (CFs) in metal oxides, respectively. The CFs are formed by the metal ions transferring from the top electrode to the bottom electrode through the electrochemical metallization effect [13–15]. In previous studies, researchers have focused on the electrically manipulated conductive filament. If the magnetic structures can be manipulated at the same time, it is possible to construct multilevel memory devices for exploration. RRAM is an excellent system for controlling both electrical and magnetic properties at the same time. Therefore, the electrical manipulation of magnetic properties in RRAM is a hot issue.

* Correspondence: tengjiao@mater.ustb.edu.cn; longshibing@ime.ac.cn

¹Department of Materials Physics and Chemistry, University of Science and Technology Beijing, Beijing 100083, China

²Key Laboratory of Microelectronic Devices & Integrated Technology, Institute of Microelectronics, Chinese Academy of Sciences, Beijing 100029, China

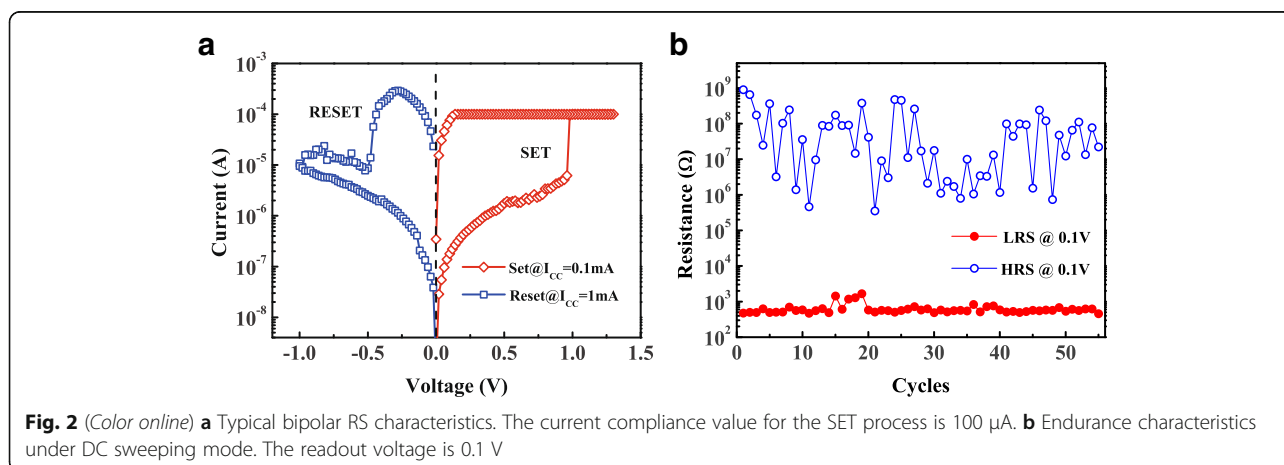
Full list of author information is available at the end of the article

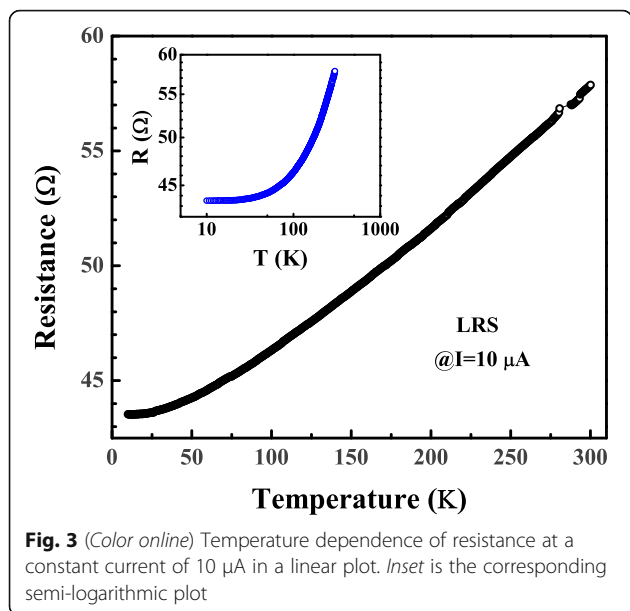


Recently, the Ni CF in RRAM has been confirmed to show ferromagnetism [16, 17]. To manipulate ferromagnetism, it is necessary to understand the magnetic structure. As different metal electrodes have obvious influence on the resistive switching behaviors [18], the magnetic structure characteristics in the RRAM devices with different magnetic electrodes such as Fe, Co, or Fe might be different. On the other hand, direct characterization of the magnetic structure is very difficult. Actually, anisotropic magnetoresistance (AMR) [19, 20] is a good method not only to confirm the ferromagnetism but also to give detailed magnetic structure information. HfO_2 is a widely used resistive switching dielectric which has been demonstrated to show excellent memory performances [21, 22]. Co conductive filament has been proved to be formed in the oxide-based RRAM device using Co as an active metal electrode [23]. Therefore, in this study, we fabricated a kind of CBRAM device with Co/ HfO_2 /Pt structure to investigate the magnetic structure characteristics of the filament in the device. We measured the AMR by rotating the direction of the magnetic field and by sweeping the magnitude, respectively. In this way, we obtained the spatial direction as well as the easy-axis of the CF.

Methods

The fabricated device has a simple crossbar structure formed on a thermally oxidized Si substrate, as shown in Fig. 1a. The size of cross section is from 5×5 to $30 \times 30 \mu m^2$. Figure 1b illustrates the cross section of the Co/ HfO_2 /Pt structure. First, sequential Ti/Pt layers (5/30 nm) were deposited by direct current (DC) magnetron sputtering as adhesion layer and bottom electrode. Then, a HfO_2 (30 nm) layer was deposited on the Pt electrode by radio frequency (RF) magnetron sputtering. Finally, a Co layer (50 nm) was deposited by DC magnetron sputtering as the top electrode and a Pt layer (10 nm) was covered on Co layer to prevent oxidation of Co. The electrical measurements are performed by Keithley 4200-SCS Semiconductor Characterization System at 300 K in atmosphere with DC voltage sweeping mode. The bias polarity is defined with reference to the bottom Pt electrode. In the forming and SET switching, a current compliance of 0.1 mA is limited to prevent the complete dielectric breakdown. By using the Physical Property Measurement System (PPMS), AMR of CF in LRS was measured at 300, 200, 100, and 10 K by rotating the direction of the magnetic field and by sweeping the magnitude, respectively. Figure 1c shows the schematic of resistance network of the device and the electrodes. A





four-probe method was used during the measurements of the LRS state and AMR. In the HRS, a two-probe method was used during measurements because resistance of the HRS is much greater than that of electrodes.

Results and Discussion

The device was operated under positive SET and negative RESET operation mode, suggesting the bipolar switching mechanism. Figure 2a shows the typical bipolar RS characteristic of the Co/HfO₂/Pt devices. As the positive bias is applied to the Co electrode, the current increases abruptly at ~ 1 V, which indicates that a transition from HRS to LRS occurs, corresponding to the SET process. When the bias with the opposite polarity is applied, the current decreases abruptly to a low value, which corresponds to the RESET process. The device switches reversibly between HRS and LRS under the DC voltages in alternative polarities. The conductive filament model accounts for the switching mechanism of

the device. Figure 2b shows the endurance of RS behavior in DC voltage sweeping mode, where the read voltage is 0.1 V. RS phenomena with a high HRS/LRS ratio can be observed.

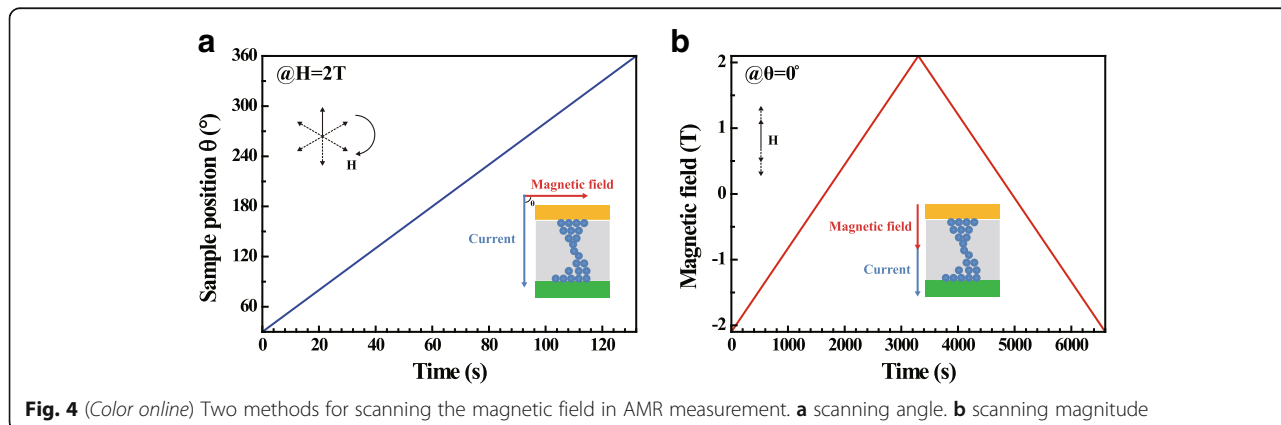
Figure 3 shows the resistance dependent temperature of the conductive filament in LRS. The resistance of the LRS decreases almost linearly as the temperature is lowered from 280 to 50 K, indicating that the CF has a metallic conduction property. The residual resistivity ratio (RRR), which can be expressed as $\text{RRR} = R_{300\text{ K}}/R_{10\text{ K}}$ is 1.33. This value is much smaller than that of the bulk pure Co. It is suggested that the conductive electrons in the CF are scattered by lattice imperfections such as surfaces, grain boundaries, and impurities [24, 25].

From the above results, it has been found that the ferromagnetic conductive filament has been formed in the RRAM, but the magnetic structure of the filaments is unclear. To examine the magnetic characteristics of CF, we measured the AMR in two methods as shown in Fig. 4. The first measurement method is fixing the magnitude of the magnetic field at 2 T, and rotating its direction continuously from 0° to 360° (Fig. 4a). The second method is fixing the direction of the magnetic field and scanning its magnitude between +2 T and -2 T. The direction is fixed as $\theta = 0^\circ$ as shown in Fig. 4b, i.e., the magnetic field is perpendicular to the substrate and the Co top electrode planes.

AMR is given by

$$\rho(\theta) = \rho_{\perp} \sin^2\theta + \rho_{\parallel} \cos^2\theta \tag{1}$$

where θ is the angle between the current in the material, and the direction of the magnetization, ρ_{\perp} and ρ_{\parallel} are the electrical resistivities perpendicular and parallel to the direction of magnetization, respectively. In the case of ferromagnetic transition metals and alloys, ρ_{\parallel} is the maximum of the $\rho(\theta)$, and ρ_{\perp} is the minimum of the $\rho(\theta)$. Figure 5 shows the resistance as a function of the angle between the current and the magnetic field



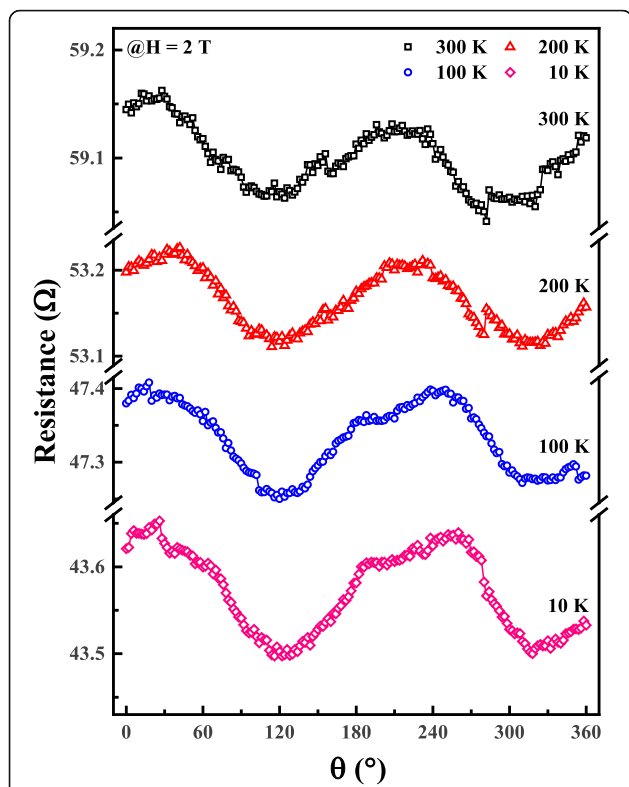


Fig. 5 (Color online) The magnetoresistance varying as a function of sample angle at different temperatures. The direction and magnitude of the magnetic field are the same as those in Fig. 4a. The inflow of constant current is 10 μ A to read the resistance

directions at different temperatures. As can be seen from the black curve in Fig. 5, ρ_{\parallel} appears at about 30° and ρ_{\perp} presents at about 120° . The results indicate that when the direction of electric current in the CF is tilted by about 30° from the magnetic field direction, the magnetoresistance is the maximum. In the measurement of as shown in Fig. 5, the applied magnetic field is large enough and greater than the saturation field, indicating that the magnetization direction tends to be parallel to the direction of the applied magnetic field. When the maximum of ρ appears, the magnetization direction is parallel to the electric current direction. Meanwhile, the angle between the z axis and the magnetic field direction is 30° , which means the angle between the z axis and the magnetization direction is 30° . Therefore, the angle between the z axis and the current direction is 30° .

Concave AMR curves were observed under the sweeping magnetic field with $\theta = 0^{\circ}$ at different temperatures, as shown in Fig. 6. When the magnetic field sweeps forth and back, the magnetoresistance curves have two different concave peaks at each fixed temperature, indicating that the easy-axis of the CF is along with the direction of the external magnetic field perpendicular to the top electrode plane. As mentioned above, the maximum of ρ in Fig. 5 appears when the magnetization direction is parallel to the electric current direction, which corresponds to ρ_{\parallel} . The maximum of ρ in Fig. 6a) appearing at $H = 0$ is close to ρ_{\parallel} . It means that the direction of

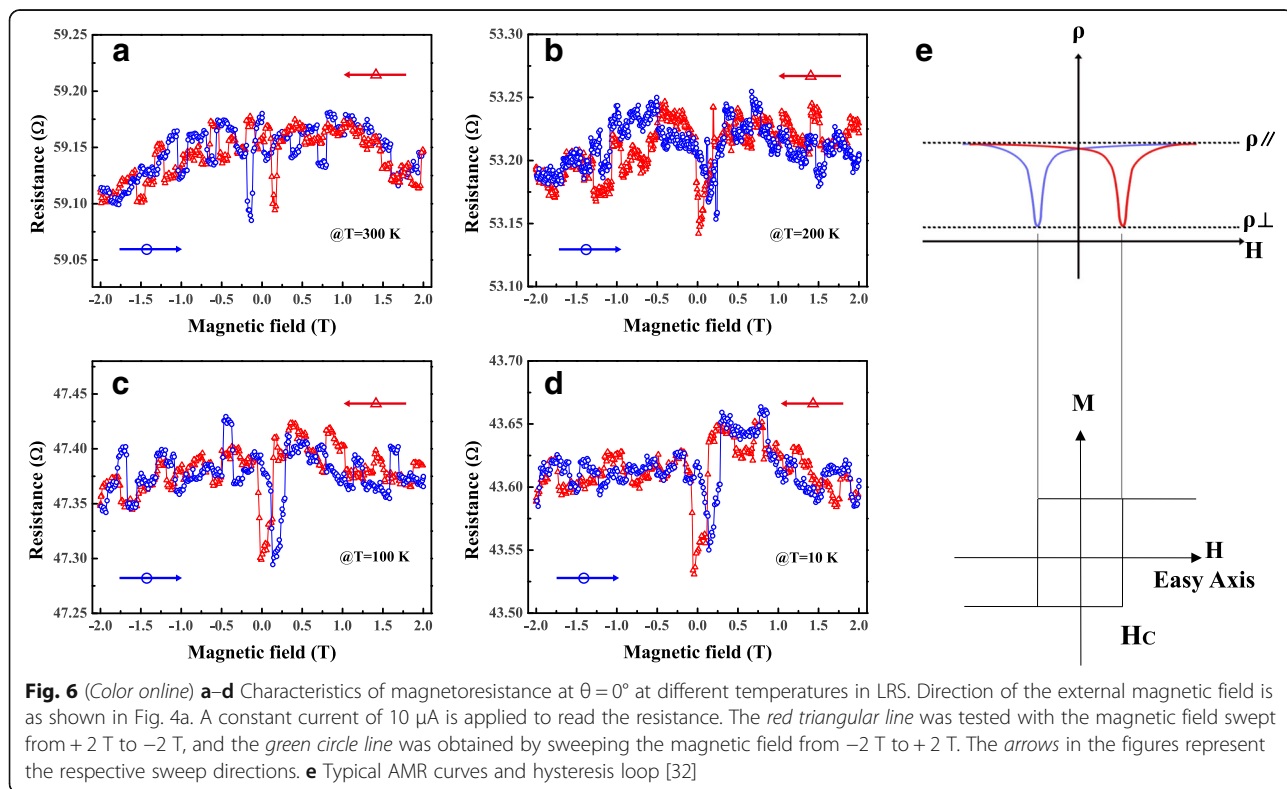


Fig. 6 (Color online) **a–d** Characteristics of magnetoresistance at $\theta = 0^{\circ}$ at different temperatures in LRS. Direction of the external magnetic field is as shown in Fig. 4a. A constant current of 10 μ A is applied to read the resistance. The *red triangular line* was tested with the magnetic field swept from +2 T to –2 T, and the *green circle line* was obtained by sweeping the magnetic field from –2 T to +2 T. The *arrows* in the figures represent the respective sweep directions. **e** Typical AMR curves and hysteresis loop [32]

magnetization at zero field is approximately parallel to the direction of electric current, indicating the out-of-plane magnetic anisotropy of the CF. The downward peaks correspond to the position of coercivity, as shown in Fig. 6e.

The fabricated device with ferromagnetic CF exhibits both electric field-induced resistive switching and magnetic field-induced magnetoresistance properties. Although the observed magnitude of AMR is small, there is the possibility of obtaining a large MR, such as using a transistor to achieve a stable current limit to precisely control the size of the magnetic conductive filament. When the size of the magnetic channel is less than the average free path of electrons, ballistic transport will occur, thus large MR effect might be obtained [26–30]. Furthermore, in the low-temperature environment, the quantum effect will become more significant [31]. We expect that the ferromagnetic CF will pave the way to a new multi-functional device with both spin-dependent and electrical field-dependent conduction properties, not only for memory but also for logic device functions as well.

Conclusions

We investigated the resistive switching characteristics of the ferromagnetic CF in RRAM device with a Co/HfO₂/Pt structure. Bipolar switching was observed. The temperature dependence of the resistance of the CF formed in the device exhibits metallic conduction properties. It was shown that AMR occurs in the LRS, which strongly suggests that a ferromagnetic CF is formed in the HfO₂ layer. Through analyzing the AMR phenomenon produced by the conductive filament, the maximum magnetoresistance appears when angle between the direction of magnetic field and that of the electric current in the CF is about 30°, while the easy-axis of the CF is along the direction perpendicular to the top electrode plane.

Abbreviations

AMR: Anisotropic magnetoresistance; CBRAM: Conductive bridge random access memory; CF: Conductive filament; ECM: Electrochemical metallization memory; HRS: High resistance states; LRS: Low resistance states; PPMS: Physical property measurement system; RRAM: Resistive random access memory; RS: Resistive switching

Acknowledgements

This work was supported by the National Natural Science Foundation of China (NSFC) under Grant Nos. 61322408, 61521064, 61574169, 61334007, 61274091, 61422407, 61522048, 61474136, 61474007, 61574166 and 61376112, the Ministry of Science and Technology of China under Grant Nos. 2016YFA0201803, 2016YFA0203800, and 2014AA032900, the Beijing Training Project For the Leading Talents in S&T under Grant No. Ijrc201508, the Chinese Academy of Sciences under Grant No. QYZDY-SSW-JSC001, the Opening Project of Key Laboratory of Microelectronics Devices & Integrated Technology, Institute of Microelectronics of Chinese Academy of Sciences.

Authors' Contributions

SL and JT designed and conducted all the experiments. LL fabricated samples. LL and QG carried out the experimental measurement. LL and YL

wrote the manuscript. All authors critically read and contributed to the manuscript preparation. All authors read and approved the final manuscript.

Competing Interests

The authors declare that they have no competing interests.

Publisher's Note

Springer Nature remains neutral with regard to jurisdictional claims in published maps and institutional affiliations.

Author details

¹Department of Materials Physics and Chemistry, University of Science and Technology Beijing, Beijing 100083, China. ²Key Laboratory of Microelectronic Devices & Integrated Technology, Institute of Microelectronics, Chinese Academy of Sciences, Beijing 100029, China. ³Nanoscale Physics & Devices Laboratory, Institute of Physics, Chinese Academy of Sciences, Beijing 100190, China. ⁴University of Chinese Academy of Sciences, Beijing 100049, China. ⁵Jiangsu National Synergetic Innovation Center for Advanced Materials (SICAM), Nanjing 210023, China.

Received: 29 December 2016 Accepted: 6 March 2017

Published online: 22 March 2017

References

- Waser R, Dittmann R, Staikov C, Szot K (2009) Redox-based resistive switching memories nanoionic mechanisms, prospects, and challenges. *Adv Mater* 21:2632–63. doi:10.1002/adma.200900375
- Yang Y, Gao P, Gaba S et al (2012) Observation of conducting filament growth in nanoscale resistive memories. *Nat Commun* 3:732–8. doi:10.1038/ncomms1737
- Zhang M, Long S, Wang G, et al (2014) Statistical characteristics of reset switching in Cu/HfO₂/Pt resistive switching memory. 9:1–7. doi: 10.1186/1556-276X-9-694
- Wong HSP, Lee HY, Yu S et al (2012) Metal-oxide RRAM. *Proc IEEE* 100:1951–70. doi:10.1109/JPROC.2012.2190369
- Jana D, Dutta M, Samanta S, Maikap S (2014) RRAM characteristics using a new Cr/GdOx/TiN structure. *Nanoscale Res Lett* 9:1–9. doi:10.1186/1556-276X-9-680
- Chang T, Jo SH, Lu W (2011) Short-term memory to long-term memory transition in a nanoscale memristor. *ACS Nano* 5:7669–76. doi:10.1021/nn202983n
- Pi S, Ghadiri-Sadrabadi M, Bardin JC, Xia Q (2015) Nanoscale memristive radiofrequency switches. *Nat Comm* 6:7519. doi:10.1038/ncomms8519
- Akinaga H, Shima H (2010) Resistive Random Access Memory (ReRAM): A Metal Oxide Memory Cell. *Proc IEEE*, to be Publ 1–36. doi: 10.1109/JPROC.2010.2070830
- Pan F, Gao S, Chen C et al (2014) Recent progress in resistive random access memories: materials, switching mechanisms, and performance. *Mater Sci Eng R Reports* 83:1–59. doi:10.1016/j.mser.2014.06.002
- Chang K-C, Chang T-C, Tsai T-M et al (2015) Physical and chemical mechanisms in oxide-based resistance random access memory. *Nanoscale Res Lett* 10:120. doi:10.1186/s11671-015-0740-7
- Tsuruoka T, Terabe K, Hasegawa T, Aono M (2010) Forming and switching mechanisms of a cation-migration-based oxide resistive memory. *Nanotechnology* 21:425205. doi:10.1088/0957-4484/21/42/425205
- Valov I, Sapezanskaia I, Nayak A et al (2012) Atomically controlled electrochemical nucleation at superionic solid electrolyte surfaces. *Nat Mater* 11:530–5. doi:10.1038/nmat3307
- Tian X, Yang S, Zeng M et al (2014) Bipolar electrochemical mechanism for mass transfer in nanoionic resistive memories. *Adv Mater* 26:3649–54. doi: 10.1002/adma.201400127
- Valov I, Waser R, Jameson JR, Kozicki MN (2011) Electrochemical metallization memories—fundamentals, applications, prospects. *Nanotechnology* 22:254003. doi:10.1088/0957-4484/22/28/289502
- Yang JJ, Strukov DB, Stewart DR (2013) Memristive devices for computing. *Nat Nanotechnol* 8:13–24. doi:10.1038/nnano.2012.240
- Otsuka S, Hamada Y, Shimizu T, Shingubara S (2014) Ferromagnetic nano-conductive filament formed in Ni/TiO₂/Pt resistive-switching memory. *Appl Phys A Mater Sci Process* 118:613–9. doi:10.1007/s00339-014-8769-5

17. Otsuka S, Hamada Y, Ito D et al (2015) Magnetoresistance of conductive filament in Ni/HfO₂/Pt resistive switching memory. *Jpn J Appl Phys* 54: 05ED02. doi:10.7567/JJAP.54.05ED02
18. Xue WH, Xiao W, Shang J et al (2014) Intrinsic and interfacial effect of electrode metals on the resistive switching behaviors of zinc oxide films. *Nanotechnology* 25(42):425204. doi:10.1088/0957-4484/25/42/425204
19. McGuire T, Potter RL (1975) Anisotropic magnetoresistance in ferromagnetic 3d alloys. *IEEE Trans Magn* 11(4):1018–38. doi:10.1109/TMAG.1975.1058782
20. Smit J (1951) Magnetoresistance of ferromagnetic metals and alloys at low temperatures. *Physica* 17(6):612–27. doi:10.1016/0031-8914(51)90117-6
21. Shang J, Liu G, Yang H et al (2014) Thermally stable transparent resistive random access memory based on all-oxide heterostructures. *Adv Funct Mater* 24(15):2171–9. doi:10.1002/adfm.201470093
22. Long S, Perniola L, Cagli C, et al (2013) Voltage and power-controlled regimes transition of HfO₂-based RRAM. *Sci Rep* 1–8. doi: 10.1038/srep02929
23. Yang Z, Zhan Q, Zhu X et al (2014) Tunneling magnetoresistance induced by controllable formation of Co filaments in resistive switching Co/ZnO/Fe structures. *Europhys Lett* 108(5):58004. doi:10.1209/0295-5075/108/58004
24. Okamoto K, Tada M, Sakamoto T et al (2011) Conducting mechanism of atom switch with polymer solid-electrolyte. *Tech Dig - Int Electron Devices Meet IEDM* 1:279–82. doi:10.1109/IEDM.2011.6131538
25. Rheem Y, Yoo BY, Beyermann WP, Myung NV (2007) Magneto-transport studies of single ferromagnetic nanowire. *Phys Status Solidi Appl Mater Sci* 204:4004–8. doi:10.1002/pssa.200777135
26. Li Q, Shen T-T, Cao Y-L et al (2014) Spin memristive magnetic tunnel junctions with CoO-ZnO nano composite barrier. *Sci Rep* 4:3835. doi:10.1038/srep03835
27. Sokolov A, Sabirianov R, Sabirianov I, Doudin B (2009) Voltage-induced switching with magnetoresistance signature in magnetic nano-filaments. *J Phys Condens Matter* 21:485303. doi:10.1088/0953-8984/21/48/485303
28. Teixeira JM, Ventura J, Fermento R et al (2009) Electroforming, magnetic and resistive switching in MgO-based tunnel junctions. *J Phys D Appl Phys* 42:105407. doi:10.1088/0022-3727/42/10/105407
29. Zhang Z, Jiang L (2014) Bias voltage induced resistance switching effect in single-molecule magnets' tunneling junction. *Nanotechnology* 25:365201. doi:10.1088/0957-4484/25/36/365201
30. Pertsev N a, Kohlstedt H (2010) Resistive switching via the converse magnetoelectric effect in ferromagnetic multilayers on ferroelectric substrates. *Nanotechnology* 21:475202. doi:10.1088/0957-4484/21/47/475202
31. Hu C, Teng J, Yu G et al (2015) Conditions for quantized anisotropic magnetoresistance. *Phys Rev B - Condens Matter Mater Phys* 91:1–5. doi:10.1103/PhysRevB.91.045438
32. Robert CO, Handley O (2000) *Modern magnetic materials: principles and applications*

Submit your manuscript to a SpringerOpen[®] journal and benefit from:

- Convenient online submission
- Rigorous peer review
- Immediate publication on acceptance
- Open access: articles freely available online
- High visibility within the field
- Retaining the copyright to your article

Submit your next manuscript at ► springeropen.com
